

Ratio of Products of Mixture Gamma Variates with Applications to Wireless Communications

Hussien Al-Hmood, Rafed Sabbar Abbas, and H. S. Al-Raweshidy

Abstract—In this paper, the statistical properties of the product of independent and non-identically distributed mixture Gamma (MG) random variables (RVs) are provided first. Specifically, simple exact closed-form expressions for the probability density function (PDF), cumulative distribution function (CDF), and moment generating function (MGF) are derived in terms of univariate Meijer's G -function. The statistical characterisations of the distribution of the ratio of products of MG variates are then derived. These statistics are used to analyse the outage probability (OP), the average error probability for different modulation schemes, the effective rate (ER) of communications systems and the average area under the receiver operating characteristics (AUC) curve of energy detection over cascaded fading channels. Additionally, the lower bound of secure outage probability (SOP^L) and probability of non-zero secrecy capacity (PNSC) of the physical layer and the OP of the multihop communications systems with decode-and-forward (DF) relaying protocol and co-channel interference (CCI) are studied by utilising the statistics of the ratio of the products. The derived performance metrics are applied for the Beaulieu-Xie and $\alpha - \lambda - \eta - \mu$ shadowed fading channels that have not been yet investigated in the literature. Accordingly, the equivalent parameters of a MG distribution for the aforementioned channels are given. A comparison between the numerical results and the Monte Carlo simulations is presented to verify the validation of our analysis.

Index Terms—Mixture gamma distribution, ratio of products, outage probability, error rate probability, effective rate, physical layer security, Beaulieu-Xie, $\alpha - \lambda - \eta - \mu$ shadowed.

I. INTRODUCTION

THE performance of several wireless communications systems can be analysed via using the statistics of the distribution of products of the random variables (RVs) and ratio of products of the variates. For instance, the statistical properties of products of RVs can be employed for cascaded fading channels, multihop transmission with non-regenerative relays [1], multi-antenna systems operating in the presence of keyholes [2], and vehicle-to-vehicle (V2V) communications [3]. In addition, the performance of wireless communications systems in the presence of co-channel interference (CCI) [4] and physical layer security (PLS) [5] can be investigated by the ratio of products of RVs.

Based on above practical usefulness, many efforts have been devoted in the open technical literature to derive the distribution of products of RVs using various fading models. For instance, in [6], the statistical properties, namely, the probability density function (PDF), the cumulative distribution function (CDF), and the moment generating function (MGF), of product of N independent and non-identically distributed (i.n.i.d.) Nakagami- m variates were derived. In [7], the PDF of the product of independent Rayleigh variates was accurately approximated to be expressed in terms of elementary

functions such as power and exponential. Simple approximate expressions for the PDF and CDF of the cascaded independent Rayleigh, generalised Gamma, Nakagami- m , Gaussian, and Weibull fading channels were given in [8]. The statistical characterisations of the product of i.n.i.d. squared generalised- K (K_G) variates were presented in [9] with applications to the orthogonal space-time block codes (STBC) over multiple-input multiple-output (MIMO) keyhole K_G fading channels.

On the other hand, different distributions of ratio of products of RVs have been analysed by the previous works. For example, the performances of the maximal ratio combining (MRC) diversity reception and multi-carrier code-division multiple access (MC-CDMA) system affected by an interference were studied in [10] by using the statistics of independent and identically distributed (i.i.d.) exponential variates. In [11], the ratios of products of Gamma and Weibull RVs were analysed. The distribution of some mathematical operations, such as, products, powers, and ratios, of arbitrary H -function variates that can be used as a unified representation for a large number of fading channels, was derived in [12].

Recently, the products of generalised $\alpha - \mu$, $\kappa - \mu$, $\eta - \mu$, [13]–[18], and Fisher-Snedecor \mathcal{F} [5], [19] RVs, have been given a special attention by many studies in the literature. This is because these distributions give better fitting to the practical data and provide various composite multipath/shadowing fading conditions. Moreover, these distributions unify most of the well-known classic fading conditions where they include Rayleigh, Nakagami- m , Rician, exponential distributions as special cases. Additionally, the $\alpha - \mu$ fading channel can be used to model the non-linear environment of communication systems whereas the $\kappa - \mu$ and the $\eta - \mu$ fading channels can be employed to represent the line-of-sight (LoS) and the non-LoS (NLoS) scenarios, respectively. Hence, the PDF, the CDF, and the MGF of the product of two i.n.i.d. $\alpha - \mu$ and $\kappa - \mu$ variates and their applications to double and composite fading channels were analysed in [13] and [14], respectively. In [15], the statistics of non-identical cascaded $\alpha - \mu$ fading channels were given in terms of Fox's H -function and applied in the analysis of the lower bound of secure outage probability (SOP^L) and probability of non-zero secrecy capacity (PNSC) of the PLS. The products of two envelopes that are modelled by $\alpha - \mu$, $\kappa - \mu$, and $\eta - \mu$ distributions were investigated in [16] via providing infinite series expressions and closed-form results in terms of multivariate Fox's H -function (FHF). The statistical characterisations of independent but not necessarily identically distributed N cascaded Fisher-Snedecor \mathcal{F} fading channels that are composite of Nakagami- m /inverse Nakagami- m distributions, were studied in [17].

For the ratio of products, the PDF and the CDF of i.n.i.d. $\alpha - \mu$ variates were explained in [18]. Similar to the mathematical results of [16], the statistics of the ratio of two envelopes taken from $\alpha - \mu$, $\kappa - \mu$, and $\eta - \mu$ RVs were given in [19] and employed in the analysis of the PNSC of the PLS over different combined non-identical fading conditions of V2V communications. In the same context, the statistical properties of the distribution of ratio of products of i.n.i.d. Fisher-Snedecor \mathcal{F} fading channels were derived in [5] in terms of single variable Meijer's G -function and applied in studying the performance of the PLS and full-duplex (FD) relaying systems with CCI.

In this paper, we derive the statistical properties of the distribution of ratio of products of i.n.i.d. mixture Gamma (MG) variates that have not been yet provided by the previous work. The MG distribution has been widely utilised as a highly accurate approximation for large numbers of fading models [20]-[25]. For instance, in [20], the outage probability (OP), the average bit error probability (ABEP), the average channel capacity (ACC), and the performance of energy detection (ED) over Nakagami- m , $\kappa - \mu$, and $\eta - \mu$ fading channels were first analysed using a MG distribution. The average detection probability (ADP) and average area under the receiver operating characteristics (AUC) curve of ED over $\alpha - \mu$ /Gamma, $\kappa - \mu$ /Gamma, and $\eta - \mu$ /Gamma fading channels were studied in [21]. Furthermore, unified analysis of the channel capacity under different transmission protocols and the effective rate (ER) of communications systems over $\alpha - \eta - \mu$ /Gamma fading conditions were investigated in [22] and [23], respectively. The performance of the PLS over MG distribution based model of both main and wire-tap channels were reported in [24] and [25]. The sum and the maximum of i.i.d. K_G and i.n.i.d. $\eta - \mu$ /gamma fading channels were derived in [26] and [27], respectively, using a MG distribution with applications to the selection combining (SC) and the MRC diversity receptions.

The main contributions of this work are summarised as follows

- We derive exact closed-form computationally tractable expressions of the PDF, the CDF, and the MGF of the distribution of products of i.n.i.d. MG variates in terms of a single variable Meijer's G -function. To the best of the authors' knowledge, these unified statistics have not been yet reported in the open technical literature.
- Based on the above results, novel statistical properties of ratio of products of i.n.i.d. MG variates are provided in simple exact closed-form expressions.
- The equivalent parameters of a MG distribution for Beaulieu-Xie [28] and $\alpha - \lambda - \eta - \mu$ shadowed fading channels [29] that are not available in the open literature, are derived. Additionally, the analysis of these fading channels via utilising the exact PDF of a single RV which would lead to mathematically intractable statistical properties due to its including the modified Bessel function of the first kind.
- Capitalising on the above statistics, the OP, the ABEP, the average symbol error probability (ASEP) for different modulation schemes, and the ER of communications systems and the average AUC of ED over non-identical

cascaded fading channels are given in exact closed-form expressions. To the best of the authors knowledge, both the performance metrics ER and the average AUC of ED over cascaded fading channels have not been yet analysed by the previous works.

- We utilise the CDF of the ratio of products to obtain the OP of multihop communications systems with decode-and-forward (DF) relaying protocol and subject to multiple interferers, the SOP^L , and PNSC of the PLS. Unlike [30] in which the SOP^L and PNSC over Beaulieu-Xie fading channels are expressed in terms of infinite series, our derived results are given in simple exact closed-form expressions.

The rest of the paper is organized as follows. Section II explains a preliminary information about a MG distribution. Section III is divided into two Subsections A and B. In the former, the statistical properties of products of MG variates are derived whereas in the latter, the statistics of ratio of products of MG RVs are given. The equivalent parameters of a MG distribution for Beaulieu-Xie and $\alpha - \lambda - \eta - \mu$ shadowed fading channels are provided in Section IV. Based on the results of Section III.A, some performance metrics of wireless communications systems over cascaded fading channels are derived in Section V whereas Section VI uses the expressions of Section III.B for some applications of wireless communications systems. The numerical results are presented in Section VII. Finally, some conclusions are highlighted in Section VIII.

II. MG DISTRIBUTION BASED CHANNEL MODEL

The PDF of the instantaneous signal-to-noise ratio (SNR) at i th path, γ_i , using a MG distribution is expressed as [20, eq. (1)]

$$f_{\gamma_i}(\gamma) = \sum_{l_i=1}^{L_i} \sigma_{l_i} \gamma^{\beta_{l_i}-1} e^{-\zeta_{l_i} \gamma} \quad (1)$$

where L_i stands for the number of terms of l th Gamma component with parameters σ_{l_i} , β_{l_i} , and ζ_{l_i} . According to [20], the minimum number of terms, L_i , that can provide a good matching between the approximate and exact distributions can be computed by using the mean square error (MSE) between the PDF of these distributions.

III. RATIO OF PRODUCTS OF MG VARIATES

In this section, the PDF, the CDF, and the MGF of the distribution of products i.n.i.d. MG variates are derived first. The results are then extended to obtain the statistics of ratio of products of i.n.i.d. MG RVs.

A. Product of i.n.i.d. MG Variates

Theorem 1: Let $Y \triangleq \prod_{i=1}^N \gamma_i$, where $\gamma_i \sim \text{MG}(L_i, \sigma_{l_i}, \beta_{l_i}, \zeta_{l_i})$ for $i = 1, \dots, N$ are i.n.i.d. MG-distributed RVs.

The PDF, the CDF, and the MGF of Y can be respectively derived as

$$f_Y(y) = \sum_{l_1=1}^{L_1} \cdots \sum_{l_N=1}^{L_N} \Phi_N G_{0,N}^{N,0} \left[\Xi_N y \middle| (\beta_{l_i} - 1)_{i=1:N} \right], \quad (2)$$

$$F_Y(y) = \sum_{l_1=1}^{L_1} \cdots \sum_{l_N=1}^{L_N} \frac{\Phi_N}{y^{-1}} G_{1,N+1}^{N,1} \left[\Xi_N y \middle| (\beta_{l_i} - 1)_{i=1:N}, -1 \right], \quad (3)$$

$$\mathcal{M}_Y(s) = \sum_{l_1=1}^{L_1} \cdots \sum_{l_N=1}^{L_N} \frac{\Phi_N}{s} G_{1,N}^{N,1} \left[\frac{\Xi_N}{s} \middle| (\beta_{l_i} - 1)_{i=1:N} \right], \quad (4)$$

where $\Phi_N = \prod_{i=1}^N \frac{\sigma_{l_i}}{\zeta_{l_i}^{\beta_{l_i}-1}}$, $\Xi_N = \prod_{i=1}^N \zeta_{l_i}$ and $G_{p,q}^{a,b}[\cdot]$ is the Meijer's G -function defined in [31, eq. (1.112)].

Proof: The Mellin transform of Y , $\mathbf{M}_Y(n)$, can be expressed as

$$\mathbf{M}_Y(n) = \prod_{i=1}^N \mathbf{M}_{\gamma_i}(n). \quad (5)$$

where $\mathbf{M}_{\gamma_i}(n)$ is the Mellin transform of the PDF of γ_i that can be evaluated by [31, eq. (2.1)]

$$\mathbf{M}_{\gamma_i}(n) = \int_0^\infty \gamma^{n-1} f_{\gamma_i}(\gamma) d\gamma. \quad (6)$$

Substituting (1) into (4) and using [30, eq. (3.381.4)], this yields

$$\mathbf{M}_{\gamma_i}(n) = \sum_{l_i=1}^{L_i} \sigma_{l_i} \zeta_{l_i}^{1-n-\beta_{l_i}} \Gamma(\beta_{l_i} - 1 + n). \quad (7)$$

where $\Gamma(a) = \int_0^\infty x^{a-1} e^{-x} dx$ is the incomplete Gamma function [32, eq. (8.310.1)].

Now, plugging (7) in (5) to obtain the following multiple summation expression

$$\mathbf{M}_Y(n) = \sum_{l_1=1}^{L_1} \cdots \sum_{l_N=1}^{L_N} \Phi_N \Xi_N^{-n} \prod_{i=1}^N \Gamma(\beta_{l_i} - 1 + n). \quad (8)$$

Inserting (8) in (5) and recalling [33, eq. (1.20)], we have

$$f_Y(y) = \sum_{l_1=1}^{L_1} \cdots \sum_{l_N=1}^{L_N} \Phi_N \times \frac{1}{2\pi i} \int_{\mathcal{L}} \left(\prod_{i=1}^N \Gamma(\beta_{l_i} - 1 + t) \right) (\Xi_N y)^{-t} dt. \quad (9)$$

where $i = \sqrt{-1}$, and \mathcal{L} is the suitable contours in the t -plane from $\varrho - i\infty$ to $\varrho + i\infty$ with ϱ is a constant value.

With the help of [31, eq. (1.112)], (9) can be written in exact closed-form as given in (2) which completes the proof of the PDF.

The CDF of Y that is given in (3) can be deduced after substituting (2) into $F_Y(y) = \int_0^y f_Y(y) dy$ and invoking [31, eq. (2.53)].

The MGF of Y can be obtained via inserting (2) in $\mathcal{M}_Y(s) = \int_0^\infty e^{-sy} f_Y(y) dy$ and using [31, eq. (2.29)] which

finishes the proof. ■

B. Ratio of Products of i.n.i.d. MG Variates

Theorem 2: Assume $X \triangleq \frac{Y}{Z}$ where $Y = \prod_{i=1}^N \gamma_{1,i}$ and $Z = \prod_{j=1}^M \gamma_{2,j}$ where $\gamma_{1,i} \sim \text{MG}(L_{1,i}, \sigma_{l_{1,i}}, \beta_{l_{1,i}}, \zeta_{l_{1,i}})$ for $i = 1, \dots, N$ and $\gamma_{2,j} \sim \text{MG}(L_{2,j}, \sigma_{l_{2,j}}, \beta_{l_{2,j}}, \zeta_{l_{2,j}})$ for $j = 1, \dots, M$ are i.n.i.d. MG-distributed RVs. Accordingly, The PDF, the CDF, and the MGF of X can be respectively deduced as follows

$$f_X(x) = \sum_{i=1, \dots, N}^{L_i} \sum_{j=1, \dots, M}^{L_j} \frac{\Phi_N \Phi_M}{\Xi_M^2} \times G_{M,N}^{N,M} \left[\frac{\Xi_N}{\Xi_M} x \middle| (\beta_{r_j})_{j=1:M}, (\beta_{l_i} - 1)_{i=1:N} \right], \quad (10)$$

$$F_X(x) = \sum_{i=1, \dots, N}^{L_i} \sum_{j=1, \dots, M}^{L_j} \frac{\Phi_N \Phi_M}{\Xi_M^2} x \times G_{M+1,N+1}^{N,M+1} \left[\frac{\Xi_N}{\Xi_M} x \middle| (\beta_{r_j})_{j=1:M}, 0, (\beta_{l_i} - 1)_{i=1:N}, -1 \right], \quad (11)$$

$$\mathcal{M}_X(s) = \sum_{i=1, \dots, N}^{L_i} \sum_{j=1, \dots, M}^{L_j} \frac{\Phi_N \Phi_M}{\Xi_M^2 s} \times G_{M+1,N}^{N,M+1} \left[\frac{\Xi_N}{s \Xi_M} \middle| (\beta_{r_j})_{j=1:M}, 0, (\beta_{l_i} - 1)_{i=1:N} \right], \quad (12)$$

Proof: Using the same methodology that is given in Proposition 1 to compute the Mellin transform for both Y and Z . Thereafter, plugging the result in $\mathbf{M}_X(n) = \mathbf{M}_Y(n) \mathbf{M}_Z(2-n)$ to obtain

$$\mathbf{M}_X(n) = \sum_{i=1, \dots, N}^{L_i} \Phi_N \Xi_N^{-n} \left(\prod_{i=1}^N \Gamma(\beta_{l_i} - 1 + n) \right) \sum_{j=1, \dots, M}^{L_j} \Phi_M \Xi_M^{-(2-n)} \left(\prod_{j=1}^M \Gamma(\beta_{r_j} + 1 - n) \right). \quad (13)$$

Substituting (13) into [33, eq. (1.21)], the PDF of X can be expressed as

$$f_X(x) = \sum_{i=1, \dots, N}^{L_i} \sum_{j=1, \dots, M}^{L_j} \frac{\Phi_N \Phi_M}{\Xi_M^2} \times \frac{1}{2\pi i} \int_{\mathcal{L}} \left(\frac{\Xi_N}{\Xi_M} x \right)^{-t} \left(\prod_{i=1}^N \Gamma(\beta_{l_i} - 1 + n) \right) \left(\prod_{j=1}^M \Gamma(\beta_{r_j} + 1 - n) \right) dt. \quad (14)$$

With the aid of the definition of Meijer's G -function [31, eq. (1.112)], (14) can be expressed in exact closed-form as shown in (10) and the proof is accomplished.

Following the similar steps of deriving (3) and (4) that are provided in Proposition 1, the CDF and the MGF of X can be deduced as given in (11) and (12), respectively, which completes the proof. ■

IV. MODELLING OF FADING CHANNELS USING A MG DISTRIBUTION

A. Beaulieu-Xie Fading Channels

The Beaulieu-Xie fading model is proposed as a simple representation for multiple specular and diffuse scatter components via introducing a special scale for the non-central chi-distribution [28]. Moreover, this model unifies the non-central chi, $\kappa - \mu$, and generalized Rician distributions where the relationship between the latter and Beaulieu-Xie distributions is the same as that between the Nakagami- m and Rayleigh models. Additionally, the Beaulieu-Xie distribution is related to the Nakagami- m model in a similar relationship that is between the Rician and Rayleigh fading models [28].

The PDF of γ_i , $f_{\gamma_i}(\gamma)$, over Beaulieu-Xie fading channel can be derived after employing [28, eq. (4)] and performing simple change of variables. Thus, this yields

$$f_{\gamma_i}(\gamma) = \frac{2^{\frac{m_i-1}{2}} m_i^{\frac{m_i+1}{2}} e^{-\frac{\lambda_i^2}{2}}}{\lambda_i^{m_i-1} \bar{\gamma}_i^{\frac{m_i+1}{2}}} \gamma^{\frac{m_i-1}{2}} e^{-\frac{m_i}{\bar{\gamma}_i} \gamma} \times I_{m_i-1} \left(\lambda_i \sqrt{\frac{2m_i \gamma}{\bar{\gamma}_i}} \right). \quad (15)$$

where $\bar{\gamma}_i$ is the average SNR, m_i is the fading parameter, λ_i controls the location and the height of the PDF, and $I_{m_i-1}(\cdot)$ is the modified Bessel function of the first kind and $m_i - 1$ order. When $m_i = 1$, the Beaulieu-Xie fading model reduces to Rician distribution with factor $K_i = \lambda_i / \Omega_i$ where Ω_i controls the spread of the PDF whereas the Rayleigh fading is obtained after plugging $m_i = 1$ and $K_i = 0$.

With the aid of the identity [32, eq. (8.445)], the modified Bessel function of (15) can be written as

$$I_{m_i-1} \left(\lambda_i \sqrt{\frac{2m_i \gamma}{\bar{\gamma}_i}} \right) = \sum_{l_i=1}^{\infty} \frac{1}{\Gamma(l_i) \Gamma(m_i + l_i - 1)} \left(\lambda_i \sqrt{\frac{2m_i \gamma}{\bar{\gamma}_i}} \right)^{2l_i + m_i - 3}. \quad (16)$$

Plugging (16) in (15), we have

$$f_{\gamma_i}(\gamma) = \sum_{l_i=1}^{\infty} \frac{\lambda_i^{2(l_i-1)} e^{-\frac{\lambda_i^2}{2}} \left(\frac{2m_i}{\bar{\gamma}_i} \right)^{m_i+l_i-2}}{\Gamma(l_i) \Gamma(m_i + l_i - 1)} \gamma^{m_i+l_i-2} e^{-\frac{m_i}{\bar{\gamma}_i} \gamma}. \quad (17)$$

It can be noted that the infinite series of (16) can be approximated to the number of terms, L_i , that satisfies the required accuracy of the MSE. Accordingly, by matching the PDF of (17) with that of (15), the equivalent parameters of a

MG for the Beaulieu-Xie fading channel are expressed as

$$\beta_{l_i} = m_i + l_i - 1, \quad \sigma_{l_i} = \frac{\theta_{l_i}}{\sum_{j_i=1}^{L_i} \theta_{j_i} \Gamma(\beta_{j_i}) \zeta_{j_i}^{-\beta_{j_i}}}$$

$$\zeta_{l_i} = \frac{m_i}{\bar{\gamma}_i}, \quad \theta_{l_i} = \frac{\lambda_i^{2(l_i-1)} e^{-\frac{\lambda_i^2}{2}}}{\Gamma(l_i) \Gamma(m_i + l_i - 1)} \left(\frac{2m_i}{\bar{\gamma}_i} \right)^{m_i+l_i-2}. \quad (18)$$

B. $\alpha - \lambda - \eta - \mu$ Shadowed Fading Channels

The $\alpha - \lambda - \eta - \mu$ shadowed fading channel is a composite model of $\alpha - \lambda - \eta - \mu$ and Nakagami- m distributions. The $\alpha - \lambda - \eta - \mu$ is proposed in [29] as a generalised distribution that unifies the $\alpha - \mu$, $\lambda - \mu$, and $\eta - \mu$ fading models. Hence, this fading model can be employed to represent the non-linear medium and the non-line-of-sight (NLoS) environment of the wireless communications. Furthermore, the $\alpha - \lambda - \eta - \mu$ shadowed can be used to model a wide range of composite multipath/shadowed fading scenarios such as $\alpha - \mu$ /Nakagami- m , $\lambda - \mu$ /Nakagami- m , and $\eta - \mu$ /Nakagami- m [21]. However, the PDF of the $\alpha - \lambda - \eta - \mu$ distribution is included the modified Bessel function which would lead to results that are expressed in terms of a non-analytical mathematically complicated functions or include an infinite series. Hence, a MG distribution is used in this effort to approximate the PDF of the composite $\alpha - \lambda - \eta - \mu$ /Nakagami- m .

The PDF of γ_i , $f_{\gamma_i}(\gamma)$, over $\alpha - \lambda - \eta - \mu$ fading channel is given as [29, eq. (10)]

$$f_{\gamma_i}(\gamma) = \psi_i \gamma^{\phi_i-1} e^{-\rho_i \gamma^{\frac{\alpha_i}{2}}} I_{\mu_i-\frac{1}{2}}(\vartheta_i \gamma^{\frac{\alpha_i}{2}}). \quad (19)$$

where $\psi_i = \frac{\sqrt{\pi} \alpha_i (\mu_i (1 + \eta_i^{-1}))^{\mu_i + \frac{1}{2}}}{\Gamma(\mu_i) a_i^{\mu_i - \frac{1}{2}} \bar{\gamma}_i^{\frac{\alpha_i}{2} (\mu_i + \frac{1}{2})}} \left(\frac{\eta_i}{1 - \lambda_i^2} \right)^{\mu_i}$ with $a_i = \frac{\sqrt{(\eta_i - 1)^2 + 4\eta_i \lambda_i^2}}{1 - \lambda_i^2}$, $\phi_i = \frac{\alpha_i}{2} (\mu_i + \frac{1}{2})$, $\rho_i = \frac{\mu_i (1 + \eta_i)^2}{2\eta_i (1 - \lambda_i^2) \bar{\gamma}_i^{\alpha_i/2}}$, and $\vartheta_i = \frac{a_i \mu_i (1 + \eta_i)}{2\eta_i \bar{\gamma}_i^{\alpha_i/2}}$. The fading parameters are defined as follows, α_i stands for the non-linearity parameter, λ_i denotes the correlation coefficient between the quadrature components and in-phase scattered waves, η_i indicates the ratio between the power of the quadrature and in-phase scattered components, and μ_i represents the real extension of the multipath clusters.

The PDF of Nakagami- m distribution is expressed as

$$f_{x_i}(x) = \frac{m_i^{m_i}}{\Gamma(m_i)} x^{m_i-1} e^{-m_i x}. \quad (20)$$

where m_i refers to the shadowing severity index in this work.

According to [13, eq. (4)], the PDF of the product of two RVs can be evaluated by

$$f_{\gamma_i}(\gamma) = \int_0^{\infty} \frac{1}{r} f_{\gamma_i} \left(\frac{\gamma}{r} \right) f_{x_i}(r) dr. \quad (21)$$

Substituting (19) and (20) into (21), this obtains

$$f_{\gamma_i}(\gamma) = \frac{\psi_i m_i^{m_i}}{\Gamma(m_i)} \gamma^{\phi_i-1} \times \int_0^{\infty} r^{m_i-\phi_i-1} e^{-\rho_i \frac{\gamma^{\alpha_i/2}}{r^{\alpha_i/2}} - m_i r} I_{\mu_i-\frac{1}{2}} \left(\vartheta_i \frac{\gamma^{\alpha_i/2}}{r^{\alpha_i/2}} \right) dr. \quad (22)$$

Using the substitution $z = \rho_i \frac{\gamma^{\alpha_i/2}}{r^{\alpha_i/2}}$ into (22), this yields

$$f_{\gamma_i}(\gamma) = \frac{2\psi_i m_i^{m_i}}{\alpha_i \Gamma(m_i)} \rho_i^{\frac{2(m_i - \phi_i)}{\alpha_i}} \gamma^{\phi_i - 1} \int_0^\infty e^{-z} g(z) dz. \quad (23)$$

where $g(z) = z^{1 - \frac{2(m_i - \phi_i)}{\alpha_i}} e^{-m_i \frac{\rho_i^{2/\alpha_i}}{z^{2/\alpha_i}}} I_{\mu_i - \frac{1}{2}} \left(\frac{\vartheta_i}{\rho_i} z \right)$.

With the help of a Gaussian-Laguerre quadrature approximation, the integration in (23), $\Lambda = \int_0^\infty e^{-z} g(z) dz$, can be expressed as $\Lambda \approx \sum_{l_i=0}^{L_i} w_{l_i} g(z_{l_i})$, where w_{l_i} and z_{l_i} are respectively the weight factors and abscissas defined in [34]. Consequently, (23) can be rewritten using (1) with the following parameters

$$\begin{aligned} \beta_{l_i} &= m_i, \quad \zeta_{l_i} = m_i \frac{\rho_i^{2/\alpha_i}}{z_{l_i}^{2/\alpha_i}}, \quad \sigma_{l_i} = \frac{\theta_{l_i}}{\sum_{j_i=1}^{L_i} \theta_{j_i} \Gamma(\beta_{j_i}) \zeta_{j_i}^{-\beta_{j_i}}} \\ \theta_{l_i} &= \frac{2\psi_i m_i^{m_i}}{\alpha_i \Gamma(m_i)} w_{l_i} \rho_i^{\frac{2(m_i - \phi_i)}{\alpha_i}} z_{l_i}^{1 - \frac{2(m_i - \phi_i)}{\alpha_i}} I_{\mu_i - \frac{1}{2}} \left(\frac{\vartheta_i}{\rho_i} z_{l_i} \right). \end{aligned} \quad (24)$$

V. APPLICATIONS OF PRODUCTS OF MG RVs TO CASCADED FADING CHANNELS

A. Outage Probability

The OP is an important performance metric of the wireless communication systems operating over fading channels and its defined as the probability that the output SNR drops below a predefined threshold value γ_{th} [35]. Accordingly, the OP of the cascaded fading channels that are modelled by a MG distribution, can be calculated by [35, eq. (1.4)]

$$P_o = F_Y(\gamma_{th}). \quad (25)$$

where $F_Y(\cdot)$ is given in (3).

B. Average Bit and Symbol Error Probability

In this section, the ABEP and the ASEP for several modulation schemes over cascaded fading channels that are represented by a MG distribution, are derived in exact unified closed-form expressions.

1) *Non-Coherent BFSK and DBPSK*: The ABEP of non-coherent binary frequency shift keying (NC-BFSK) and differential binary phase shift keying (DBPSK), \bar{P}_b , can be computed by [35, eq. (9.254)]

$$\bar{P}_b = \frac{\mathcal{M}_Y(g_1)}{2}. \quad (26)$$

where $g_1 = 0.5$ and $g_1 = 1$ for NC-BFSK and DBPSK, respectively, and $\mathcal{M}_Y(\cdot)$ is provided in (4).

2) *Coherent BPSK, BFSK, and BFSK with Minimum Correlation*: The ABEP of coherent BFSK, BPSK, and BFSK with minimum correlation can be evaluated by [35, eq. (9.11)]

$$\bar{P}_b^C = \frac{1}{\pi} \int_0^{\frac{\pi}{2}} \mathcal{M}_Y \left(\frac{g_2}{\sin^2 \theta} \right) d\theta. \quad (27)$$

where $g_2 = 0.5$, $g_2 = 1$, and $g_2 = 0.715$ for coherent BFSK, BPSK, and BFSK with minimum correlation, respectively.

Proposition 1: The ABEP of coherent BFSK, BPSK, and BFSK with minimum correlation, \bar{P}_b^C , over cascaded fading

conditions is obtained as

$$\begin{aligned} \bar{P}_b^C &= \frac{\Gamma(\frac{1}{2})}{2\pi g_2} \sum_{l_1=1}^{L_1} \cdots \sum_{l_N=1}^{L_N} \Phi_N \\ &\quad \times G_{2,N+1}^{N,2} \left[\frac{\Xi_N}{g_2} \middle| \begin{matrix} 0, -0.5 \\ (\beta_{l_i} - 1)_{i=1:N}, -1 \end{matrix} \right]. \end{aligned} \quad (28)$$

Proof: Plugging (4) in (27) and using the change of the variable $x = \sin^2 \theta$ with some mathematical manipulations, we have

$$\begin{aligned} \bar{P}_b^C &= \frac{1}{\pi} \sum_{l_1=1}^{L_1} \cdots \sum_{l_N=1}^{L_N} \frac{\Phi_N}{2g_2} \\ &\quad \times \int_0^1 \frac{\sqrt{x}}{\sqrt{1-x}} G_{1,N}^{N,1} \left[\frac{\Xi_N}{g_2} x \middle| \begin{matrix} 0 \\ (\beta_{l_i} - 1)_{i=1:N} \end{matrix} \right] dx. \end{aligned} \quad (29)$$

With the aid of the definition of the Meijer's G -function [31, eq. (1.112)] and the Fubini's theorem that is applied to interchange the order of the linear and closed integrations, (29) becomes

$$\begin{aligned} \bar{P}_b^C &= \frac{1}{\pi} \sum_{l_1=1}^{L_1} \cdots \sum_{l_N=1}^{L_N} \frac{\Phi_N}{2g_2} \frac{1}{2\pi i} \int_{\mathcal{L}} \int_0^1 \frac{x^{\frac{1}{2}-t}}{\sqrt{1-x}} dx \\ &\quad \times \Gamma(1-t) \left(\prod_{i=1}^N \Gamma(\beta_{l_i} - 1 + t) \right) \left(\frac{\Xi_N}{g_2} \right)^{-t} dt. \end{aligned} \quad (30)$$

It can be noted that the inner integral of (30) can be computed as

$$\int_0^1 \frac{x^{\frac{1}{2}-t}}{\sqrt{1-x}} dx \stackrel{(a)}{=} B \left(\frac{1}{2}, \frac{3}{2} - t \right). \quad (31)$$

where $B(\cdot, \cdot)$ is the Beta function defined in [32, eq. (8.380.1)] and (a) follows [32, eq. (3.191.3)].

Recalling the property [32, eq. (8.384.1)] for (31) and inserting the result in (30) which completes the proof of (28). ■

3) *M-PSK*: The ASEP of M -PSK can be calculated by [35, eq. (9.15)]

$$\bar{P}_s^{M-PSK} = \frac{1}{\pi} \int_0^{\pi - \frac{\pi}{M}} \mathcal{M}_Y \left(\frac{g_{PSK}}{\sin^2 \theta} \right) d\theta. \quad (32)$$

where $g_{PSK} = \sin^2 \frac{\pi}{M}$ with $M = 4, 8, 16, \dots$.

Proposition 2: The ASEP of M -PSK over cascaded fading channels using a MG distribution is given in (33) shown at the top of the next page. In (33), $G_{c,d;c_1,d_1;c_2,d_2}^{a,b;a_1,b_1;a_2,b_2}[\cdot]$ is the bivariate Meijer's G -function defined in [36, eq. (10)].

Proof: After performing simple mathematical manipulations, (32) can be rewritten as

$$\begin{aligned} \bar{P}_s^{M-PSK} &= \overbrace{\frac{2}{\pi} \int_0^{\frac{\pi}{2}} \mathcal{M}_Y \left(\frac{g_{PSK}}{\sin^2 \theta} \right) d\theta}^{\mathcal{I}_1} \\ &\quad - \underbrace{\frac{1}{\pi} \int_0^{\frac{\pi}{M}} \mathcal{M}_Y \left(\frac{g_{PSK}}{\sin^2 \theta} \right) d\theta}_{\mathcal{I}_2}. \end{aligned} \quad (34)$$

One can see that \mathcal{I}_1 can be evaluated by following the same methodology of the Proposition 3 as provided in the first term

$$\begin{aligned} \bar{P}_s^{M-PSK} = \sum_{l_1=1}^{L_1} \cdots \sum_{l_N=1}^{L_N} \frac{\Phi_N}{g_{PSK}} \left\{ \frac{\Gamma(\frac{1}{2})}{\pi} G_{2,N+1}^{N,2} \left[\frac{\Xi_N}{g_{PSK}} \middle| \begin{matrix} 0, -0.5 \\ (\beta_{l_i} - 1)_{i=1:N}, -1 \end{matrix} \right] \right. \\ \left. - \frac{g_{PSK}^{\frac{3}{2}}}{2} G_{1,1:N,N;1,1}^{0,1:N,1;1,0} \left[\Xi_N, g_{PSK} \middle| \begin{matrix} -0.5 : 0 & ; 0.5 \\ -1.5 : (\beta_{l_i} - 1)_{i=1:N}; 0 \end{matrix} \right] \right\}. \end{aligned} \quad (33)$$

$$\begin{aligned} \bar{P}_s^{M-QAM} = \sum_{l_1=1}^{L_1} \cdots \sum_{l_N=1}^{L_N} \frac{2c\Phi_N}{g_{QAM}} \left\{ \frac{\Gamma(\frac{1}{2})}{\pi} G_{2,N+1}^{N,2} \left[\frac{\Xi_N}{g_{QAM}} \middle| \begin{matrix} 0, -0.5 \\ (\beta_{l_i} - 1)_{i=1:N}, -1 \end{matrix} \right] \right. \\ \left. - \frac{c}{\sqrt{8}} G_{1,1:N,N;1,1}^{0,1:N,1;1,0} \left[\frac{\Xi_N}{2g_{QAM}}, 0.5 \middle| \begin{matrix} -0.5 : 0 & ; 0.5 \\ -1.5 : (\beta_{l_i} - 1)_{i=1:N}; 0 \end{matrix} \right] \right\}. \end{aligned} \quad (42)$$

of (33).

For \mathcal{I}_2 , we substitute (4) in (34) and assume $x = \sin^2 \theta$, to obtain

$$\begin{aligned} \mathcal{I}_2 = \frac{\Gamma(\frac{1}{2})}{2\pi g_{PSK}} \sum_{l_1=1}^{L_1} \cdots \sum_{l_N=1}^{L_N} \Phi_N \\ \times \int_0^{g_{PSK}} \frac{\sqrt{x}}{\sqrt{1-x}} G_{1,N}^{N,1} \left[\frac{\Xi_N}{g_{PSK}} x \middle| \begin{matrix} 0 \\ (\beta_{l_i} - 1)_{i=1:N} \end{matrix} \right] dx. \end{aligned} \quad (35)$$

Using the definition of the Meijer's G -function [31, eq. (1.112)] and the Fubini's theorem, the following integral is deduced

$$\begin{aligned} \mathcal{I}_2 = \frac{\Gamma(\frac{1}{2})}{2\pi g_{PSK}} \sum_{l_1=1}^{L_1} \cdots \sum_{l_N=1}^{L_N} \Phi_N \frac{1}{2\pi i} \int_{\mathcal{L}} \int_0^{g_{PSK}} \frac{x^{\frac{1}{2}-t}}{\sqrt{1-x}} dx \\ \times \Gamma(1-t) \left(\prod_{i=1}^N \Gamma(\beta_{l_i} - 1 + t) \right) \left(\frac{\Xi_N}{g_{PSK}} \right)^{-t} dt. \end{aligned} \quad (36)$$

The inner integral of (36) can be expressed as

$$\begin{aligned} \int_0^{g_{PSK}} \frac{x^{\frac{1}{2}-t}}{\sqrt{1-x}} dx \stackrel{(b_1)}{=} \frac{g_{PSK}^{\frac{3}{2}-t}}{\frac{3}{2}-t} {}_2F_1 \left(\frac{3}{2}-t, \frac{1}{2}; \frac{5}{2}-t; g_{PSK} \right) \\ \stackrel{(b_2)}{=} \frac{\pi g_{PSK}^{\frac{3}{2}-t}}{\Gamma(\frac{1}{2})} G_{3,3}^{1,2} \left[g_{PSK} \middle| \begin{matrix} t-0.5, 0.5, 0.5 \\ 0, t-1.5, 0.5 \end{matrix} \right]. \end{aligned} \quad (37)$$

where ${}_2F_1(.,.;.)$ is the hypergeometric function defined in [32, eq. (9.14.1)]. Step (b_1) follows [32, eq. (8.391)] whereas (b_2) obtains after using the identities [32, eq. (8.331.1)] and [37, eq. (07.23.26.0005.01)] with some mathematical simplifications.

Recalling [31, eq. (1.112)] for the Meijer's G -function of (37) and substituting the result into (36) to yield

$$\begin{aligned} \mathcal{I}_2 = \frac{\sqrt{g_{PSK}}}{2} \sum_{l_1=1}^{L_1} \cdots \sum_{l_N=1}^{L_N} \Phi_N \frac{1}{(2\pi i)^2} \int_{\mathcal{L}} \int_{\mathcal{T}} \frac{\Gamma(1.5-t-r)}{\Gamma(2.5-t-r)} \\ \frac{(\prod_{i=1}^N \Gamma(\beta_{l_i} - 1 + t)) \Gamma(1-t) \Gamma(r)}{\Gamma(0.5+r)} \Xi_N^{-t} g_{PSK}^{-r} dt dr. \end{aligned} \quad (38)$$

With the aid of [36, eq. (10)], \mathcal{I}_2 can be written in exact closed-form as shown in the second term of (33) which completes the proof. ■

4) *M-QAM*: The ASEP of M -QAM can be computed by [35, eq. (9.21)]

$$\bar{P}_s^{M-QAM} = 4c(\mathcal{J}_1 - c\mathcal{J}_2) \quad (39)$$

where $c = 1 - \frac{1}{\sqrt{M}}$,

$$\mathcal{J}_1 = \frac{1}{\pi} \int_0^{\frac{\pi}{2}} \mathcal{M}_Y \left(\frac{g_{QAM}}{\sin^2 \theta} \right) d\theta \quad (40)$$

and

$$\mathcal{J}_2 = \frac{1}{\pi} \int_0^{\frac{\pi}{4}} \mathcal{M}_Y \left(\frac{g_{QAM}}{\sin^2 \theta} \right) d\theta \quad (41)$$

with $g_{QAM} = \frac{3}{2(M-1)}$ where $M = 4, 8, 16, \dots$.

It can be noted that \mathcal{J}_1 can be calculated by using the same steps of deriving \bar{P}_b^C in (28), namely, Proposition 1 as shown in the first term of (42) given at the top of this page. In addition, \mathcal{J}_2 can be derived by following the same procedure that is employed to derive \mathcal{I}_2 of (34) after inserting $M = 4$. Consequently, \bar{P}_s^{M-QAM} is obtained in exact closed-form expression as shown in (42) given at the top of this page.

C. Effective Rate of Wireless Communications Systems

The ER has been proposed to measure the performance of the wireless communications systems under the quality of service (QoS) constraints, such as system delays, that have not been neglected by Shannon theorem [38]. Hence, this performance metric has been widely analysed over different fading channels in the open technical literature (see [23] and [39] and references therein). However, there is no work has been achieved to study the ER over cascaded fading channels which is one of our contributions in this paper.

The ER, R can be calculated by [23, eq. (1)]

$$R = -\frac{1}{A} \log_2 (\mathbb{E}\{(1+y)^{-A}\}). \quad (43)$$

where $A \triangleq \theta TB / \ln 2$ with θ , T , and B are respectively the delay exponent, block duration, and bandwidth of the system and $\mathbb{E}\{\cdot\}$ stands for the expectation.

It can be noticed that (43) can be written as [39, eq. (8)]

$$R = -\frac{1}{A} \log_2 \left(\int_0^\infty (1+y)^{-A} f_Y(y) dy \right). \quad (44)$$

Now, the ER over unified cascaded fading channels using a MG distribution can be derived after inserting (2) in (44) and utilising [31, eq. (1.112)] and the Fubini's theorem. Thus, this yields

$$R = -\frac{1}{A} \sum_{l_1=1}^{L_1} \cdots \sum_{l_N=1}^{L_N} \Phi_N \frac{1}{2\pi i} \int_{\mathcal{L}} \prod_{i=1}^N \Gamma(\beta_{l_i} - 1 + t) (\Xi_N)^{-t} \times \int_0^\infty (1+y)^{-A} y^{-t} dy dt. \quad (45)$$

Invoking [32, eq. (3.194.3)] to compute the inner integral of (45) and making use of the identity [32, eq. (8.384.1)] and [31, eq. (1.112)], the following closed-form expression of the ER is deduced

$$R = -\frac{1}{A} \log_2 \left(\sum_{l_1=1}^{L_1} \cdots \sum_{l_N=1}^{L_N} \frac{\Phi_N}{\Gamma(A)} G_{1,N+1}^{N+1,1} \left[\Xi_N \left| \begin{matrix} 0 \\ (\beta_{l_i} - 1)_{i=1:N}, A-1 \end{matrix} \right. \right] \right). \quad (46)$$

D. AUC of Energy Detection-Based Spectrum Sensing

The ED technique has been widely employed to perform the spectrum sensing in both cognitive radio (CR) and ultra-wide band (WUB) systems. This refers to its low implementation intricacy where the unlicensed user doesn't need any prior information about the licensed user [20], [21], [39]-[40]. To study the behaviour of an ED, the receiver operating characteristics (ROC) curve which plots the ADP versus the false alarm probability is utilised in many efforts. But, in some cases, this performance metric doesn't provide a clear result on the superiority of one system on the other. This is due to the intersection between the two compared curves in a specific values of ADP and false alarm probability. Based on this observation, the authors in [40] proposed the average AUC curve as another performance metric of an ED via measuring the total area under the ROC.

The average AUC, \bar{A} , can be evaluated by [39, eq. (21)]

$$\bar{A} = \int_0^\infty A(y) f_Y(y) dy. \quad (47)$$

where $A(y)$ is the AUC in additive white Gaussian noise (AWGN) environment which is expressed as [39, eq. (20)]

$$A(y) = 1 - \sum_{r=0}^{u-1} \sum_{n=0}^r \binom{r+u-1}{r-n} \frac{y^n e^{-\frac{y}{2}}}{2^{r+u+n} n!}. \quad (48)$$

where $\binom{b}{a}$ denotes the binomial coefficient.

The average AUC over cascaded fading conditions can be obtained after plugging (2) and (48) in (47) and invoking the fact that $\int_0^\infty f_Y(y) dy \triangleq 1$ and [31, eq. (2.29)]. Accordingly, we have

$$\bar{A} = 1 - \sum_{r=0}^{u-1} \sum_{n=0}^r \binom{r+u-1}{r-n} \frac{1}{2^{r+u+n} n!} \sum_{l_1=1}^{L_1} \cdots \sum_{l_N=1}^{L_N} \Phi_N G_{1,N}^{N,1} \left[\frac{\Xi_N}{2} \left| \begin{matrix} -n \\ (\beta_{l_i} - 1)_{i=1:N} \end{matrix} \right. \right]. \quad (49)$$

To the best of the authors' knowledge, (49) is new and there is no effort has been done to study the average AUC over cascaded fading channels.

VI. APPLICATIONS OF THE RATIO OF THE PRODUCTS

A. Outage Probability of Multi-Hop Wireless Communication Systems with CCI

As its explained previously in Section V.A about the importance of the OP, this performance metric is given in this section for multi-hop wireless communication systems with DF relaying and interferer at each hop. In this system, the number of hops is K and the signal-to-interference ratio at the input of r -th terminal with $r \in \{1, K-1\}$, is assumed to be $X_r = \frac{\gamma_{1,1r} \gamma_{1,2r}}{\gamma_{2,1r}}$ where $\gamma_{1,1r}$, $\gamma_{1,2r}$, and $\gamma_{2,1r}$ are the RVs that represent the impact of the fading, the shadowing, and the co-channel interference, respectively [4].

According to [4, eq. (23)], the OP of K -hop wireless communication systems, $P_o^{(K)}$, can be computed by

$$P_o^{(K)} = 1 - \prod_{r=1}^K (1 - F_{X_r}(x_{th})). \quad (50)$$

where γ_{th} is the threshold value and $F_{X_k}(\cdot)$ is the CDF that is given in (11) with $N = 2$ and $M = 1$.

Based on (49), for dual-hop, i.e., $K = 2$, the OP, $P_o^{(2)}$, is written as [4, eq. (24)]

$$P_o^{(2)} = F_{X_1}(\gamma_{th}) + F_{X_2}(\gamma_{th}) - F_{X_1}(\gamma_{th}) F_{X_2}(\gamma_{th}). \quad (51)$$

Additionally, for $K = 3$, namely, triple-hop, the OP, $P_o^{(3)}$, is expressed as [4, eq. (25)]

$$P_o^{(3)} = F_{X_1}(\gamma_{th}) + F_{X_2}(\gamma_{th}) + F_{X_3}(\gamma_{th}) - F_{X_1}(\gamma_{th}) F_{X_2}(\gamma_{th}) - F_{X_1}(\gamma_{th}) F_{X_3}(\gamma_{th}) - F_{X_2}(\gamma_{th}) F_{X_3}(\gamma_{th}) + F_{X_1}(\gamma_{th}) F_{X_2}(\gamma_{th}) F_{X_3}(\gamma_{th}). \quad (52)$$

B. Physical Layer Security

The performance of the PLS over different fading channel models has been given a special consideration by many works in the literature. This is because its able to fortify the security of the wireless link [15].

In this work, we have assumed the transmitter (**S**) communicates with the legitimate receiver (**D**) via the main channel in the presence of an eavesdropper (**E**). Therefore, the channel state information (CSI) of **D** can be known by **S** whereas a perfect knowledge of the CSI of **E** cannot be assumed at **S** and hence information-theoretic security cannot be guaranteed. Additionally, both the main and wiretap channels are supposed to be independent and undergo quasi-static fading channels that are modelled by using a MG distribution. Also, we have assumed all **S**, **D** and **E** are equipped with a single received antenna [41].

1) *Lower Bound of Secure Outage Probability:* One of the main performance measurement of the PLS is the secure outage probability (SOP) [15], [24], [25], [28]. However, its difficult to derive the SOP in a unified exact closed-form computationally tractable expression [28], [41]. Therefore, the

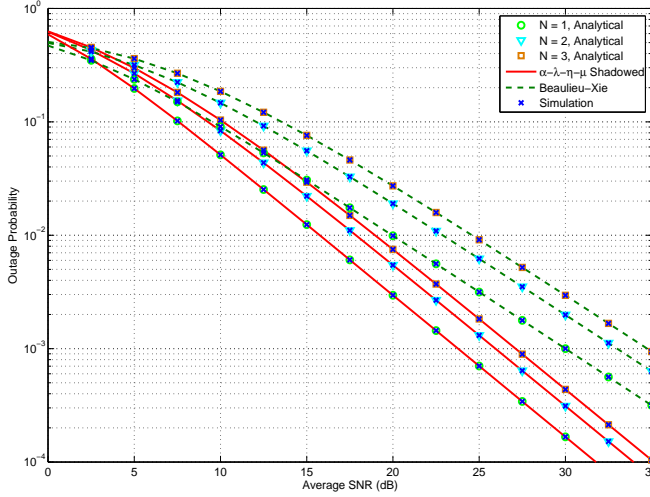


Fig. 1. OP of cascaded Beaulieu-Xie and $\alpha - \lambda - \eta - \mu$ shadowed fading channels using a MG distribution with $\gamma_{th} = 0$ dB.

lower bound of the SOP (SOP^L) is utilised in many studies in the analysis of the PLS.

The SOP^L can be evaluated by [5, eq. (39)]

$$SOP^L = F_X(\epsilon). \quad (53)$$

where $X = \frac{\gamma_D}{\gamma_E}$ which is defined in Theorem 2, γ_D and γ_E are the received SNR at **D** and **E**, respectively, $F_X(\cdot)$ is given in (11), and $\epsilon = 2^{R_{th}}$ with R_{th} denotes the target secrecy rate threshold.

In contrast to the SOP^L of [25, eq. (6)] that is given for single path and [28, eq. (27)] that is included an infinite series, (53) is derived in simple unified exact closed-form expression and can be used for the cascaded fading channels.

2) *Probability of Non-Zero Secrecy Capacity*: Another metric that is used to analyse the performance of the PLS is the PNSC which means the secrecy capacity is always positive.

The PNSC can be readily obtained from (53) as follows

$$PNSC = 1 - F_X(1). \quad (54)$$

VII. ANALYTICAL AND SIMULATION RESULTS

In this section, the numerical results of our derived expressions are compared with their Monte Carlo simulations that are obtained via running 10^6 iterations. In all figures, the minimum number of terms for i th path, L_i , that satisfies $MSE \leq 10^{-5}$ is chosen to be 15. Additionally, all paths are assumed to be independent but not necessarily identically distributed.

Fig. 1 shows the OP of cascaded Beaulieu-Xie and $\alpha - \lambda - \eta - \mu$ shadowed fading channels with $\gamma_{th} = 0$ dB for three paths, namely, $N = 1, 2$, and 3 , with $(m_1, m_2, m_3) = (1, 2, 3)$ for both fading channels. In this figure, $\lambda_1 = \lambda_2 = \lambda_3 = 0.5$ for Beaulieu-Xie fading model, whereas $\alpha_1 = \alpha_2 = \alpha_3 = 2.5$, $\lambda_1 = \lambda_2 = \lambda_3 = 0.1$, $\eta_1 = \eta_2 = \eta_3 = 0.5$, and $\mu_1 = \mu_2 = \mu_3 = 2.5$ for $\alpha - \lambda - \eta - \mu$ shadowed fading channel. For the same simulation parameters of Fig. 1, Figs. 2 and 3 compare the ABEP of BPSK with the ASEP of

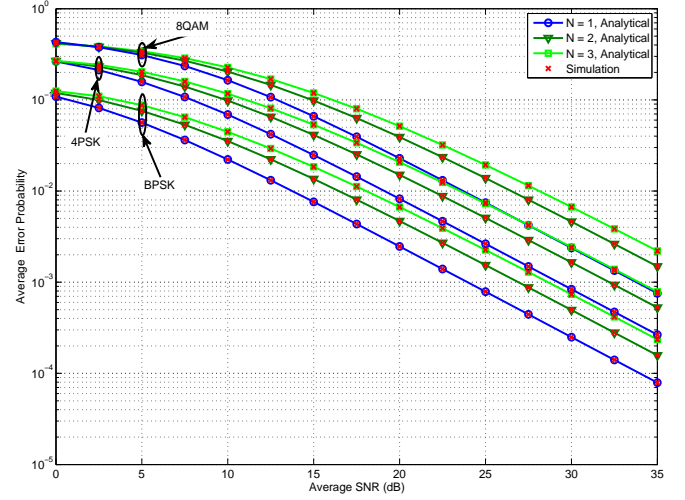


Fig. 2. ABEP of BPSK and ASEP of 4PSK and 8QAM modulation schemes over cascaded Beaulieu-Xie fading channels using a MG distribution.

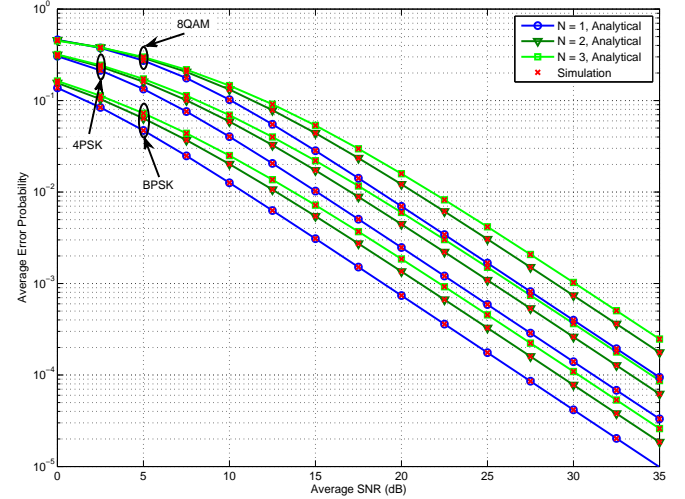


Fig. 3. ABEP of BPSK and ASEP of 4PSK and 8QAM modulation schemes over cascaded $\alpha - \lambda - \eta - \mu$ shadowed fading channels using a MG distribution.

4PSK and 8QAM modulation schemes over Beaulieu-Xie and $\alpha - \lambda - \eta - \mu$ shadowed cascaded fading channels, respectively. Figs. 4 and 5 illustrate the ER with $A = 2.5$ and the average complementary AUC which is $1 - \bar{A}$ for $u = 3$ versus the average SNR, respectively, and for the same channels parameters of Fig. 1. As anticipated and consistent with the results that are presented in [2], [4]-[19], the performance of the system decreases when the number of paths increases. This refers to the increasing in the impact of the channel parameters on the transmitted signal which becomes high when N is large. For instance, in Fig. 1, at fixed $\bar{\gamma} = 15$ dB, the values of the OP of cascaded Beaulieu-Xie and $\alpha - \lambda - \eta - \mu$ shadowed fading channels are reduced by approximately 44.89% and 43.84%, respectively, when N changes from 2 to 1. In the same context, at $N = 3$, the OP of Beaulieu-Xie fading condition is nearly 0.076 whereas for $\alpha - \lambda - \eta - \mu$ shadowed fading channels is roughly 0.029. One can see that the results

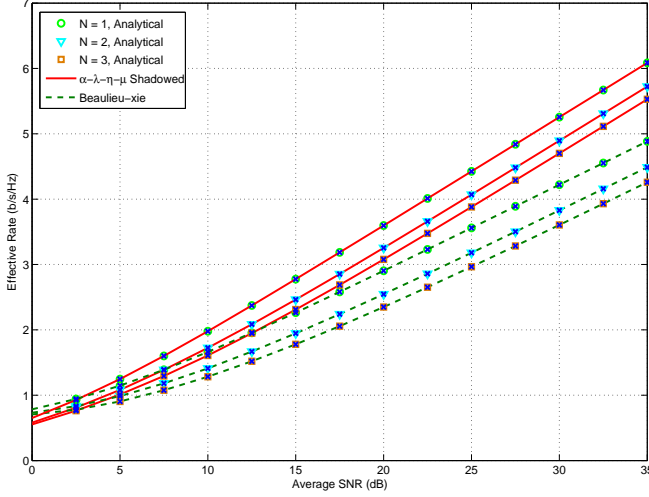


Fig. 4. ER of cascaded Beaulieu-Xie and $\alpha - \lambda - \eta - \mu$ shadowed fading channels using a MG distribution with $A = 2.5$.

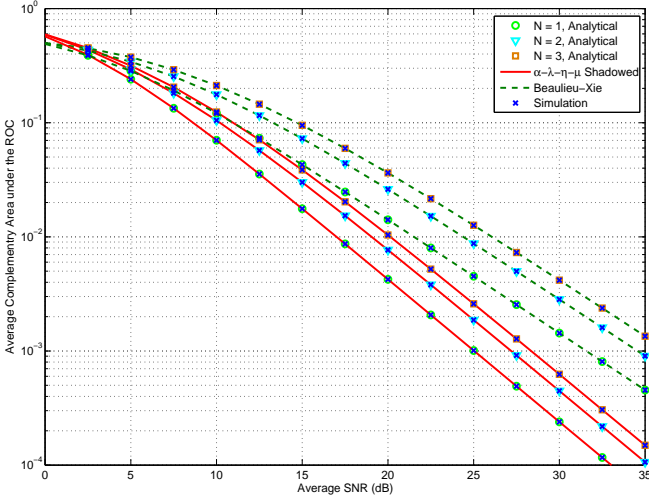


Fig. 5. Average complementary AUC of cascaded Beaulieu-Xie and $\alpha - \lambda - \eta - \mu$ shadowed fading channels using a MG distribution with $u = 3$.

of Fig. 1 have been affirmed by Figs. 2 and 3. In these figures, comparisons between the ABEP of BPSK and the ASEP of 4PSK and 8QAM modulation techniques have been carried out. Moreover, Fig. 4 explains how the cascaded fading channels affects on the quality of service (QoS) of wireless communications systems via diminishing the ER. Additionally, in Fig. 5, the average complementary AUC becomes low when the number of paths decreases. This is due to the increasing in both the missed-ADP and false alarm probability.

Fig. 6 demonstrates the OP of DF relaying based multi-hop wireless communications systems with multiple interferers for $\gamma_{th} = 0$ dB. The analysis in this figure is provided for three types of i.i.d. hops which are $K = 1$ that represents a direct link, $K = 2$, and $K = 3$ via using the same fading parameters m for both channels, and λ , α , and η of $\alpha - \lambda - \eta - \mu$ shadowed fading of Fig. 1 for all hops. However, for Beaulieu-Xie fading channels, $\lambda_1 = \lambda_2 = \lambda_3 = 0.5$ in the first hop,

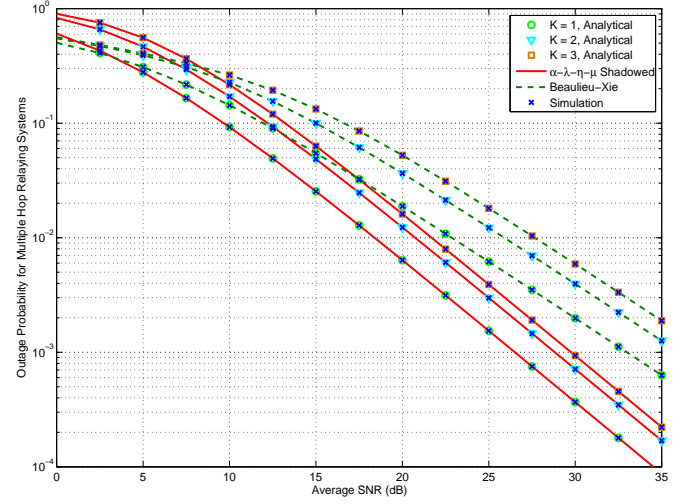


Fig. 6. OP of DF relaying based multi-hop communication systems over Beaulieu-Xie and $\alpha - \lambda - \eta - \mu$ shadowed fading channels using a MG distribution with $\gamma_{th} = 0$ dB.

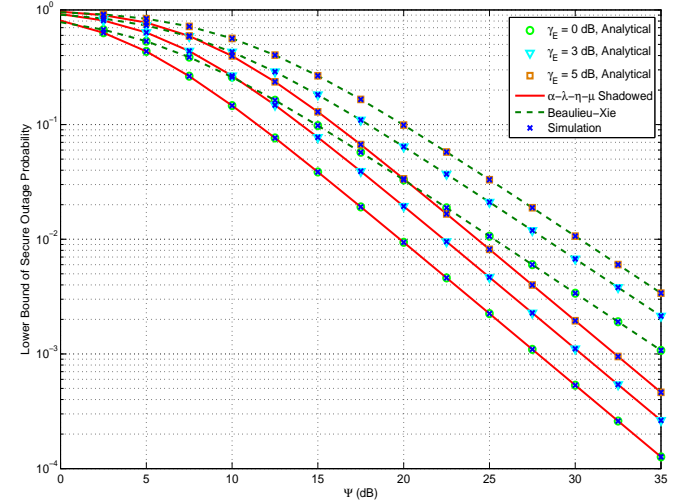


Fig. 7. SOP^L versus Ψ over Beaulieu-Xie and $\alpha - \lambda - \eta - \mu$ shadowed fading channels using a MG distribution with $R_{th} = 1$.

$\lambda_1 = \lambda_2 = \lambda_3 = 1.5$ in the second hop, and $\lambda_1 = \lambda_2 = \lambda_3 = 2.5$ in the third hop. In addition, for $\alpha - \lambda - \eta - \mu$ shadowed fading, $\mu_1 = \mu_2 = \mu_3 = 2.5$, $\mu_1 = \mu_2 = \mu_3 = 1.5$, and $\mu_1 = \mu_2 = \mu_3 = 0.5$ for the first, second, and third hops, respectively. Similar to Fig. 1, the OP drops when the number of hops, K , reduces and for both fading conditions. This observation is matched with the results that were obtained in [4].

Finally, Figs. 7 and 8 portrait the SOP^L for $R_{th} = 1$ and PNSC, respectively, versus $\Psi = \frac{\gamma_D}{\gamma_E}$ and for different values of $\bar{\gamma}_E$. For both fading channels, $m = 1$ for **D** and $m = 2$ for **E**. Besides, in Beaulieu-Xie fading channels, $\lambda = 0.5$ for both **D** and **E**. For $\alpha - \lambda - \eta - \mu$ shadowed fading, the parameters for both **D** and **E** are equal where $\alpha = 2.5$, $\lambda = 0.1$, $\eta = 0.5$, and $\mu = 2.5$. From these figures, one can notice that a substantial degradation in the secrecy performance of the system when the

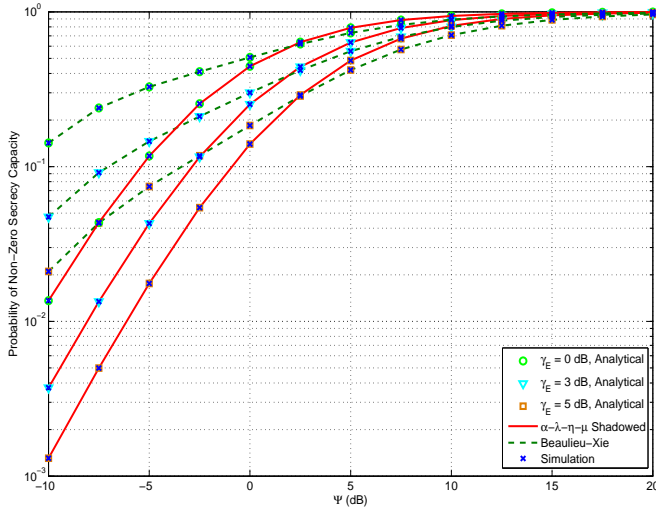


Fig. 8. PNSC versus Ψ over Beaulieu-Xie and $\alpha - \lambda - \eta - \mu$ shadowed fading channels using a MG distribution.

value of $\bar{\gamma}_E$ rises. This is because the large improvement in the wiretap channel, namely, **S-E** link in comparison with the main channel. For example, in Fig. 7 and at constant $\Psi = 10$ dB, the values of the SOP^L for $\bar{\gamma}_E = 3$ dB are higher than that of $\bar{\gamma}_E = 0$ dB by nearly 65.6% and 82.1% for Beaulieu-Xie and $\alpha - \lambda - \eta - \mu$ shadowed fading channels, respectively. This situation is consistent with the same scenarios that were analysed in [24],[25] and [41].

In all previous figures, one can observe that the numerical results are perfectly coincided with their simulation counterparts which confirms the correctness of our derived expressions.

VIII. CONCLUSIONS

In this paper, the statistical characterisations of the products of i.i.d. MG variates were derived first. Thereafter, the study was extended to include the PDF, the CDF, and the MGF of ratio of products of arbitrary distributed MG RVs. Based on these statistics, several performance metrics of wireless communications systems were analysed over cascaded Beaulieu-Xie and $\alpha - \lambda - \eta - \mu$ shadowed fading channels which have not been yet studied in the literature. In particular, the OP, the ABEP, the ASEP, the ER, and average AUC of energy detection were provided in simple unified closed-form computationally tractable expressions. Furthermore, the OP of DF relaying of multi-hop wireless communications systems with CCI and the metrics SOP^L and PNSC of the PLS were given. The numerical results for different number of paths and hops as well as the average SNR of the eavesdropper were presented and confirmed by the Monte Carlo simulations. Moreover, these results showed how the performance of the systems diminish when the aforementioned parameters are increased. The derived expressions of this work can be employed for all fading channels that were modelled by a MG distribution. Additionally, the generalisation of Beaulieu-Xie and $\alpha - \lambda - \eta - \mu$ shadowed fading channels can be exploited to analyse the behaviour of the wireless communications systems

over a wide range of fading conditions that are special cases of these channels, such as $\alpha - \lambda - \eta - \mu$ by plugging $m \rightarrow \infty$.

REFERENCES

- [1] G. K. Karagiannidis, T. A. Tsiftsis, and R. K. Mallik, "Bounds for multihop relayed communications in Nakagami- m fading," *IEEE Trans. Commun.*, vol. 54, no. 1, pp. 18-22, Jan. 2006.
- [2] K. Peppas, F. Lazarakis, A. Alexandridis, and K. Dangakis, "Cascaded generalised-K fading channel," *IET Commun.*, vol. 4, no. 1, pp. 116-124, Jan. 2010.
- [3] A.-A. A. Boulogeorgos, P. C. Sofotasios, B. Selim, S. Muhaidat, G. K. Karagiannidis, and M. Valkama, "Effects of RF impairments in communications over cascaded fading channels," *IEEE Trans. Veh. Technol.*, vol. 65, no. 11, pp. 8878-8894, Nov. 2016.
- [4] O. S. Badarneh, D. B. da Costa, M. Benjillali, and M.-S. Alouini, "Ratio of products of fluctuating two-ray variates," *IEEE Commun. Lett.*, vol. 23, no. 11, pp. 1944-1948, Nov. 2019.
- [5] H. Du, J. Zhang, K. P. Peppas, H. Zhao, B. Ai, and X. Zhang, "On the distribution of the ratio of products of Fisher-Snedecor \mathcal{F} random variables and its applications," *IEEE Trans. Veh. Technol.*, vol. 69, no. 2, pp. 1855-1866, Feb. 2020.
- [6] G. K. Karagiannidis, N. C. Sagias, and P. T. Mathiopoulos, " N^* Nakagami: A novel stochastic model for cascaded fading channels," *IEEE Trans. Commun.*, vol. 55, no. 8, pp. 1453-1458, Aug. 2007.
- [7] H. Lu, Y. Chen, and N. Cao, "Accurate approximation to the PDF of the product of independent Rayleigh random variables," *IEEE Antennas Wireless Propagat. Lett.*, vol. 10, pp. 1019-1022, Sept. 2011.
- [8] Y. Chen, G. K. Karagiannidis, H. Lu, and N. Cao, "Novel approximations to the statistics of products of independent random variables and their applications in wireless communications," *IEEE Trans. Veh. Technol.*, vol. 61, no. 2, pp. 443-454, Feb. 2011.
- [9] K. Peppas, F. Lazarakis, A. Alexandridis, and K. Dangakis, "Cascaded generalised-K fading channel," *IET Commun.*, vol. 4, no. 1, pp. 116-124, Jan. 2010.
- [10] R. Annavajjala, A. Chockalingam, and S. K. Mohammed, "On a ratio of functions of exponential random variables and some applications," *IEEE Trans. Commun.*, vol. 58, no. 11, pp. 3091-3097, Nov. 2010.
- [11] S. Nadarajah and S. Kotz, "On the product and ratio of Gamma and Weibull random variables," *Econometric Theory*, vol. 22, no. 2, pp. 338-344, Feb. 2006.
- [12] B. D. Carter and M. D. Springer, "The distribution of products, quotients and powers of independent H -function variates," *SIAM J. Appl. Math.*, vol. 33, pp. 542-558, Jul. 1977.
- [13] É. J. Leonardo, and Michel D. Yacoub, "The product of two $\alpha - \mu$ variates and the composite $\alpha - \mu$ multipath-shadowing model," *IEEE Trans. Veh. Technol.*, vol. 64, no. 6, pp. 2720-2725, June 2015.
- [14] N. Bhargav, C. R. N. da Silva, Y. J. Chun, É. J. Leonardo, S. L. Cotton, and M. D. Yacoub, "On the product of two $\kappa - \mu$ random variables and its application to double and composite fading channels," *IEEE Trans. Wireless Commun.*, vol. 17, no. 4, pp. 2457-2470, April 2018.
- [15] L. Kong, G. Kaddoum, and D. B. da Costa, "Cascaded $\alpha - \mu$ fading channels: Reliability and security analysis," *IEEE Access*, vol. 6, pp. 41978-41992, May 2018.
- [16] C. R. N. da Silva, É. J. Leonardo, and M. D. Yacoub, "Product of two envelopes taken from $\alpha - \mu$, $\kappa - \mu$, and $\eta - \mu$ distributions," *IEEE Trans. Commun.*, vol. 66, no. 3, pp. 1284-1295, Nov. 2017.
- [17] O. S. Badarneh, S. Muhaidat, P. C. Sofotasios, S. L. Cotton, K. Rabie, and D. B. da Costa, "The N^* Fisher-Snedecor \mathcal{F} cascaded fading model," in *Proc. WiMob*, Oct. 2018, pp. 1-7.
- [18] É. J. Leonardo, M. D. Yacoub, and R. A. de Souza, "Ratio of products of $\alpha - \mu$ variates," *IEEE Commun. Lett.*, vol. 20, no. 5, pp. 1022-1025, Mar. 2016.
- [19] C. R. N. da Silva, N. Simmons, É. J. Leonardo, S. L. Cotton, and M. D. Yacoub, "Ratio of two envelopes taken from $\alpha - \mu$, $\kappa - \mu$, and $\eta - \mu$ variates and some practical applications," *IEEE Access*, vol. 7, pp. 54449-54462, May 2019.
- [20] S. Atapattu, C. Tellambura, and Hai Jiang, "A mixture gamma distribution to model the SNR of wireless channels," *IEEE Trans. Wireless Commun.*, vol. 10, no. 12, pp. 4193-4203, Dec. 2011.
- [21] H. Al-Hmood and H. S. Al-Raweshidy, "Unified modeling of composite $\kappa - \mu$ /gamma, $\eta - \mu$ /gamma, and $\alpha - \mu$ /gamma fading channels using a mixture gamma distribution with applications to energy detection," *IEEE Antennas and Wireless Propagation Lett.*, vol. 16, pp. 104-108, April 2017.

- [22] H. Al-Hmood and H. S. Al-Raweshidy, "Unified analysis of channel capacity under different adaptive transmission policies," *Electronics Lett.*, vol. 56, no. 2, pp. 87-89, Jan. 2020.
- [23] H. Al-Hmood and H. S. Al-Raweshidy, "Unified approaches based effective capacity analysis over composite $\alpha - \eta - \mu$ /gamma fading channels," *Electronics Lett.*, vol. 54, no. 13, pp. 852-853, June 2018.
- [24] H. Lei, *et al.*, "Performance analysis of physical layer security over generalized- K fading channels using a mixture Gamma distribution," *IEEE Commun. Lett.*, vol. 20, no. 2, pp. 408-411, Feb. 2016.
- [25] L. Kong, G. Kaddoum, "Secrecy characteristics with assistance of mixture Gamma distribution," *IEEE Wireless Commun. Lett.*, vol. 8, no. 4, pp. 1086-1089, 2019.
- [26] J. Jung, S.-R. Lee, H. Park, S. Lee, and I. Lee, "Capacity and error probability analysis of diversity reception schemes over generalized- K fading channels using a mixture gamma distribution," *IEEE Trans. Wireless Commun.*, vol. 13, no. 9, pp. 4721-4730, Sept. 2014.
- [27] H. Al-Hmood, and H. S. Al-Raweshidy, "On the sum and the maximum of non-identically distributed composite $\eta - \mu$ /gamma variates using a mixture Gamma distribution with applications to diversity receivers," *IEEE Trans. Veh. Technol.*, vol. 65, no. 12, pp. 10048-10052, Dec. 2016.
- [28] P. S. Chauhan, S. Kumar, and S. K. Soni, "On the physical layer security over Beaulieu-Xie fading channel," *Inter. J. Electronics and Commun. (AEU)*, vol. 113, pp. 152940-152947, Jan 2020.
- [29] N. C. Beaulieu and X. Jiandong, "A novel fading model for channels with multiple dominant specular components," *IEEE Wireless Commun. Lett.*, vol. 4, no. 1, pp. 54-57, Feb. 2015.
- [30] A. K. Papazafeiropoulos, S. A. Kotsopoulos and D. Zevgolis, "The $\alpha - \lambda - \eta - \mu$: a general fading distribution," in *Proc. IEEE Wireless Commun. and Net. Conf. (WCNC)*, Budapest, 2009, pp. 1-6.
- [31] A. M. Mathai, R. K. Saxena, and H. J. Haubold, *The H-function: theory and applications*, Springer Science & Business Media, 2009.
- [32] I. S. Gradshteyn, and I. M. Ryzhik, *Table of Integrals, Series and Products*, 7th edition. Academic Press Inc., 2007.
- [33] C. D. Bodenschatz, "Finding an H-function distribution for the sum of independent H-function variates," Ph.D. dissertation, May 1992.
- [34] M. Abramowitz and I. A. Stegun, *Handbook of Mathematical Functions: With Formulas, Graphs, and Mathematical Tables*. New York, NY, USA: Dover, 1965.
- [35] M. K. Simon and M.-S. Alouini, *Digital Communication Over Fading Channels*, 2nd ed. New York, NY, USA: Wiley, 2005.
- [36] G-C. Celia, F. J. Canete, and F. J. Paris, "Capacity of $\kappa - \mu$ shadowed fading channels," *Int. J. of Antennas and Propagation*, pp.1-8, 2014.
- [37] Wolfram Research, Inc., 2020, [Online]. Available: <http://functions.wolfram.com/id>. Accessed on: May 2020.
- [38] D. Wu, and R. Negi, "Effective capacity: a wireless link model for support of quality of service," *IEEE Trans. Wireless Commun.*, vol. 2, no. 4, pp. 630-643, July 2003.
- [39] H. Al-Hmood, and H. S. Al-Raweshidy, "On the effective rate and energy detection based spectrum sensing over $\alpha - \eta - \kappa - \mu$ fading channels," *IEEE Trans. Veh. Technol.*, pp. 1-1, June 2020.
- [40] S. Atapattu, C. Tellambura, and H. Jiang, "Analysis of area under the ROC curve energy detection," *IEEE Trans. Wireless Commun.*, vol. 9, no. 3, pp. 1216-1225, Mar. 2010.
- [41] H. Al-Hmood, and H. S. Al-Raweshidy, "Performance analysis of physical-layer security over fluctuating Beckmann fading channels," *IEEE Access*, vol. 7, pp. 119541-119556, Sept. 2019.